PNAS
www.pnas.org

Supplementary Information for

Ubiquitin-dependent Switch During Assembly of the Proteasomal ATPases Mediated by Not4 Ubiquitin Ligase

Xinyi Fu[#, 1], Vladyslava Sokolova[#, 1, 2], Kristofor J Webb[1], William Old[1], and Soyeon Park*[, 1]

Soyeon Park
Email: soyeon.park-1@colorado.edu

This PDF file includes:

Supplementary text
Figs. S1 to S13
Tables S1 to S4
References for SI reference citations

www.pnas.org/cgi/doi/10.1073/pnas.1805353115

Supplementary Information Text

Supplementary Materials and Methods

Biochemical reagents, plasmids and yeast strains. A complete list of yeast strains is provided in Table S3. Antibodies to Rpt1 and Rpt6 were kind gifts from C. Mann. Antibodies to all other Rpt subunits and ubiquitin were purchased from Enzo Life Sciences. Antibodies to Nas6, Rpn1, and Ubp6 were obtained from the Finley laboratory. Anti-Nas2 antibody is a kind gift from the Roelofs laboratory. Anti-Pgk1 antibody (Life Technologies) was used as a loading control. All antibodies were used at 1:3,000 dilutions except Pgk1 (1:10,000). All biochemical and genetic experiments were performed at least twice.

Chromosomal *not4-L35A* and *not4-I64A* strains were constructed by integrating PCR-amplified *not4-L35A* and *not4-I64A* alleles into the endogenous chromosomal locus of the *NOT4*. As templates for PCR, we used plasmids from the Bielinsky laboratory and the Collart laboratory. We transformed each PCR-amplified fragment into SUB62 strain and sequence-verified their correct integration into *NOT4* locus. To construct chromosomal *rpt5-KA* (K411A, K426A, K428A) strain, we used gene synthesis service (Integrated DNA Technologies) to create the site-specific mutations, PCR-amplified the resulting DNA fragment, and then integrated it into the chromosomal locus of the *RPT5* by transformation. We sequence-verified the site-specific mutations and correct integration into *RPT5* locus.

Expression and purification of recombinant proteins. A complete list of *E. coli* strains is provided in Table S4. The chaperones were expressed in *E. coli* from pGEX6P-1 derived plasmid pJR40 (GST-Nas6), pJR56 (GST-Rpn14), pJR89 (GST-Hsm3), and pSP128 (GST-Nas2), and were purified as described (1). The GST tag was removed from each chaperone at the end of purification, using PreScission protease (1).

All Rpt full-length and truncation constructs were cloned into the pRSF-Duet1 plasmid to express N-terminal His_6-tagged proteins for purification from *E. coli*. All *E. coli* cultures were frozen as droplets into liquid nitrogen and ground into a powder using mortar and pestle as described previously (2). His_6-affinity purifications were conducted as follows. Ground powder was hydrated in lysis buffer (50mM Na-phosphate [pH 7.0], 300 mM NaCl, 10% glycerol), which was supplemented with 1 mM β-Mercaptoethanol, ATP (1 mM), and protease inhibitors. To isolate Rpt5-Rpt4 co-complex, we individually expressed His_6-tagged Rpt5 and untagged Rpt4 in *E. coli* strains and mixed the cryo-powders in equal volume. Following the hydration of the ground powder, Triton X-100 was added to 0.2% final, and samples were incubated on ice for 10 min. We then centrifuged the lysates at 20,000 x g for 30 min at 4°C, and incubated the cleared lysates with 200 µL TALON metal affinity resin (Clontech) for 1 hr at 4°C with constant rotation. Bead-bound proteins were collected by centrifugation at 3000 rpm for 5 min and washed with 15 mL of the lysis buffer containing 0.2% Triton X-100 three times. The beads were then transferred to a microspin column and were washed twice with 400 µL of lysis buffer. His-tagged proteins were eluted with 250 µL of lysis buffer containing 150 mM imidazole by rotating for 1 hr at 4°C. Eluates were dialyzed in buffer A (50 mM Tris-HCl [pH 7.0], 100 mM NaCl, 10% glycerol) overnight at 4°C.

***In vitro* ubiquitination reaction**. UBA1-3xFLAG (YYS41) was isolated from yeast, and GST-Ubc4 was expressed and purified from *E. coli* (3). Ubiquitin was purchased from Sigma (ubiquitin from bovine erythrocytes). GST-tagged Not4 was expressed and purified from *E. coli*, as described previously (4). Ubiquitination reactions were conducted in a 20 µL total volume, containing E1 (Uba1, 2 pmol), E2 (Ubc4, 100 pmol), Not4 (10 pmol), ubiquitin (1.2 nmol), ATP (2.5 mM), DTT (1 mM), an ATP regeneration system (52 mM creatine phosphate and 0.5 mg/mL creatine phosphokinase), and $MgCl_2$ (3 mM) in the proteasome buffer (specified in the following

paragraph). For this, we pre-incubated E1, E2, and ubiquitin in a 10 μL total volume for 10 min at room temperature first, and then combined this reaction with the rest of the components in a 20 μL reaction at room temperature for 1-3 hrs. For the chaperone addition experiments (Fig. 3C and 3D), we pre-incubated individual chaperones with the base for 10 min at room temperature. We then conducted ubiquitination reactions for 1 hr at room temperature. For recombinant Rpt5 proteins, ubiquitination reactions were conducted for 1.5 to 3 hr at room temperature. In all experiments, 10 μL of each sample were analyzed by 10% Bis-Tris SDS-PAGE and immunoblotting.

Affinity-purification of base and RP. The base and RP were affinity-purified from approximately 100 mL cryolysates from ProA-TEV-Rpt1 (TG931) and Rpn11-TEV-ProA (sDL133), respectively. Cryolysates were hydrated in the proteasome buffer (50 mM Tris-HCl [pH 7.5], 5 mM $MgCl_2$, 1 mM EDTA, 10% glycerol) supplemented with 1 mM ATP and incubated with 500 μL of IgG resin for 2 hrs at 4°C. We washed resin-bound complexes with 20 volumes of the proteasome buffer containing 150 mM NaCl, and then incubated them with 5 volumes of proteasome buffer containing 1M NaCl for 1 hr for the base purification (proteasome buffer containing 500 mM NaCl was used for RP purification), prior to an additional wash with 50 volumes of the same buffer at 4°C. The resulting resin-bound base and RP were washed with 10 volumes of proteasome buffer. Elution was performed with TEV protease at 0.1 unit/μL (Life Technologies) in 2 volumes of the proteasome buffer by incubating at 30°C for 1 hr. The eluates were concentrated using Amicon Ultra-0.5 centrifugal filter devices (30 kDa cut-off). ATP (1-2mM) was included throughout the entire purification procedure.

Yeast culture conditions for examination of Not4-mediated ubiquitination of Rpt5 and its impacts on the free ubiquitin levels. For affinity-purification of assembly intermediates, yeast cultures were inoculated into fresh YPD at $O.D._{600}$= 0.2 and were grown to $O.D._{600}$= 0.8 at 30°C. At this time, the cultures were diluted to $O.D._{600}$= 0.3 in 200 mL fresh YPD for further growth for 4 hrs at 37°C. To examine the free ubiquitin level, yeast cells were inoculated into fresh YPD at $O.D._{600}$=0.2 and were grown to $O.D._{600}$=0.8 at 30°C. The cultures were then diluted again to $O.D._{600}$=0.2 in 50 mL fresh YPD for further growth for 6 hrs at 37°C. In this way, yeast cells can be exposed to heat stress, in which Not4's function during chaperone-mediated proteasome assembly is prominently detectable (Fig. 2). Heat stress generates cellular misfolded proteins, which require the proteasome for their degradation. In this situation, proteasome assembly is also increased to ensure sufficient proteasome levels for increased demand for protein degradation (5). At the end of heat stress, cultures were then harvested by centrifugation at 3000 x *g* for 5 min. Cell pellets were washed with cold water, frozen in liquid nitrogen, and ground with mortar and pestle in the presence of liquid nitrogen. The resulting cryo-powders were then hydrated for further analysis as described below.

Affinity purification of endogenous chaperone-associated complexes. Yeast cultures were grown and were harvested for cryo-lysis as described in the preceding paragraph. The ground cryo-powders were hydrated with proteasome buffer (50 mM Tris-HCl [pH 7.5], 5 mM $MgCl_2$, 150 mM NaCl, 1 mM EDTA, 10% glycerol, and protease inhibitors), supplemented with 1 mM ATP. Whole cell extracts were hydrated for 10 min on ice, and centrifuged at 20,000 x *g* for 30 min at 4°C. The cleared lysates were incubated with anti-FLAG M2-agarose beads (Sigma) for 2 hrs at 4°C. The beads were washed twice with proteasome buffer containing 150 mM NaCl and ATP (1 mM), and eluted with 0.2 mg/mL FLAG peptides (Sigma) for 1 hr at 4°C. ATP was included at 1 mM throughout the purification procedure.

Growth Phenotype Assays. Overnight yeast cultures were diluted into fresh YPD media and grown to $O.D._{600}$=0.8–1.2. Three-fold serial dilutions of yeast cultures were prepared in water in 96-well plates with the highest concentration of cells equivalent to $O.D._{600}$=0.3. Cells were spotted onto plates and grown for 2-4 days. For experiments in Fig. 2B and Fig. S12A involving quadruple chaperone knockout mutants, YPD plates were supplemented with 4% casamino acid to ensure sufficient amino acid levels in these cells (6).

Sample preparation for mass spectrometry and LC-MS/MS analysis. To enrich ubiquitinated Rpt5 proteins, we conducted the Rpt5 ubiquitination reaction in 100 µL total volume. We then incubated the reactions with 10 µL of TALON metal affinity resin for 1 hr at 30°C, and removed the supernatant, which contain all other ubiquitinated proteins, including auto-ubiquitinated Not4 and the other reaction components. We then added 20 µL of Laemmlie sample buffer and boiled the samples at 95°C for 5 min. We loaded the entire samples to 10% Bis-Tris SDS-PAGE and stained with Coomassie.

Coomassie-stained gel bands were excised and cut into cubes (7). Gel pieces were destained by adding 100 µl of 1:1 100 mM ammonium bicarbonate/acetonitrile (vol/vol) for 30 min. Acetonitrile (500 µl) was added and samples were vortexed for approximately 15 min or until the gel pieces shrank and became opaque. The solution was removed and 1 µg of trypsin in 50 µl of 10 mM ammonium bicarbonate containing 10% (vol/vol) acetonitrile was added. Samples were incubated overnight at 37°C. Acetonitrile (200 µl) was added to dehydrate and extract peptides from the gel. The solution was dried in a speed-vac centrifuge. The samples were resuspended in 20 µl of 2% acetonitrile 0.1% formic acid for MS analysis.

One microliter of each sample was separated on a 0.075 × 250 mm 1.7 µM 130A C18 nanoAcquity column at 300 nL/min with an EASY-nLC 1000 UPLC system (Thermo Scientific) using mobile phases 0.1% (v/v) formic acid in liquid chromatography mass spectrometry (LCMS) water and 0.1% (v/v) formic acid in acetonitrile. The sample was analyzed with an Orbitrap Fusion (Thermo Scientific) over a 2 hr gradient. All raw files were processed using MaxQuant version 1.6.0.13(8) searching with diglycine as a variable modification at a 1% false discovery rate (FDR) at the peptide and protein levels against the SGD S288C database (version 20150113).

Deubiquitination assays. To confirm that high-molecular weight Rpt5 species are ubiquitinated Rpt5 (Fig. S9), affinity-purified assembly intermediates (2 µg) were incubated with 0.7 µL of Usp2 (Boston Biochem, Usp2 catalytic domain, amino acid residues 259-605) in 20 µL of proteasome buffer at 30°C for 45 min. To test whether Ubp6 can deubiquitinate Rpt5 (Fig. S11), affinity-purified assembly intermediates (2 µg) were incubated with recombinant Ubp6 or Ubp6-C118A (0.4 µg each) in 20 µL of proteasome buffer at 30°C for the indicated time. Ubp6 and Ubp6-C118A were expressed and purified from *E. coli* as described previously (9).

Real-time quantitative PCR. Total RNA was extracted from logarithmically growing cells, and 1 µg of total RNA was reverse transcribed to cDNA in 20 µL reaction with oligo-dT primer and a reverse transcriptase. Real-time RT-PCR was performed using iQ SYBR Green Supermix (Bio-Rad) according to manufacturer instructions.

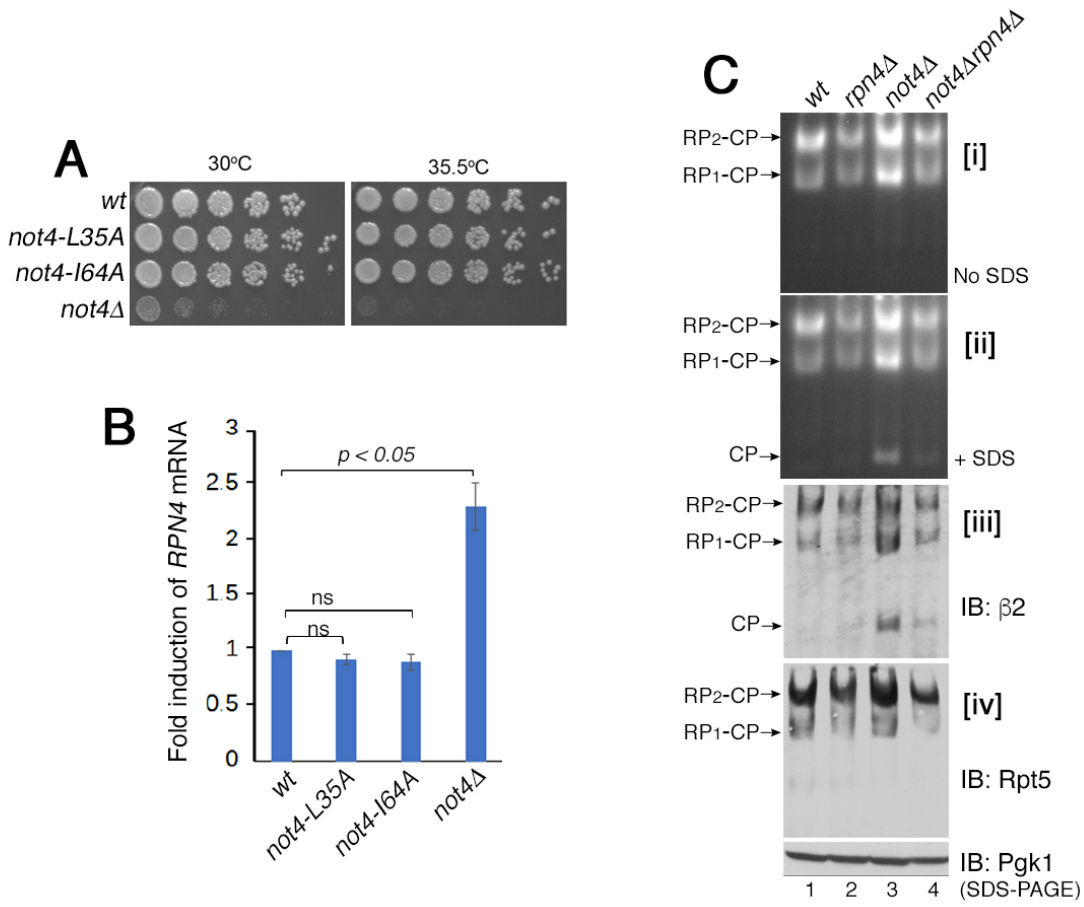

Fig. S1. The *not4Δ* mutant results in transcriptional induction of the proteasome via Rpn4, but this effect is independent of Not4's E3 ligase activity.

A, Yeast growth assays showing that the growth defect of the *not4Δ* mutant is not due to specific disruption of Not4's ubiquitin ligase activity since the *not4* catalytic point mutants (*not4-L35A* and *not4-I64A*) grow normally. Three-fold serial dilutions of indicated yeast cells were spotted onto YPD plates and grown for 3 days. Growth defects of the *not4Δ* mutant might be more related to global translation deregulation in the *not4Δ*, due to Not4's role in translation repression (10); the *not4* point mutants have no such defects.

B, Quantitative real-time PCR results showing that the mRNA level of *RPN4* is increased in the *not4Δ*, but not in the *not4-L35A* and *not4-I64A*. Rpn4 is a transcription factor that is responsible for inducible expression of all proteasome subunits (11, 12). *RPN4* mRNA is induced upon various cell stresses, including global translational deregulation in the *not4Δ* cells (10). Real-time PCR results for *RPN4* were normalized to *ACT1*. Fold induction of *RPN4* mRNA in the indicated *not4* mutants was calculated relative to wild type (average ± SEM, N=3; ns, not significant).

C, Increased proteasome levels and activities in the *not4Δ* single mutants mainly result from Rpn4-driven transcription induction since the *not4Δrpn4Δ* double mutants do not exhibit increased proteasome levels or activity (compare lane 3 to 4), but are comparable to the *rpn4Δ* single mutant (lane 2). Whole cell lysates from the indicated strains were analyzed by 3.5% native PAGE and in-gel peptidase assays using the fluorogenic peptide substrate, LLVY-AMC in the absence or presence of 0.02% SDS in [**i**] and [**ii**], respectively. Our immunoblots confirm that proteasome activities correlate with proteasome levels as shown in **[iii]**, **[iv]**. β2 is a CP subunit **[iii]**. Rpt5 is a base subunit **[iv]**. Pgk1, loading control.

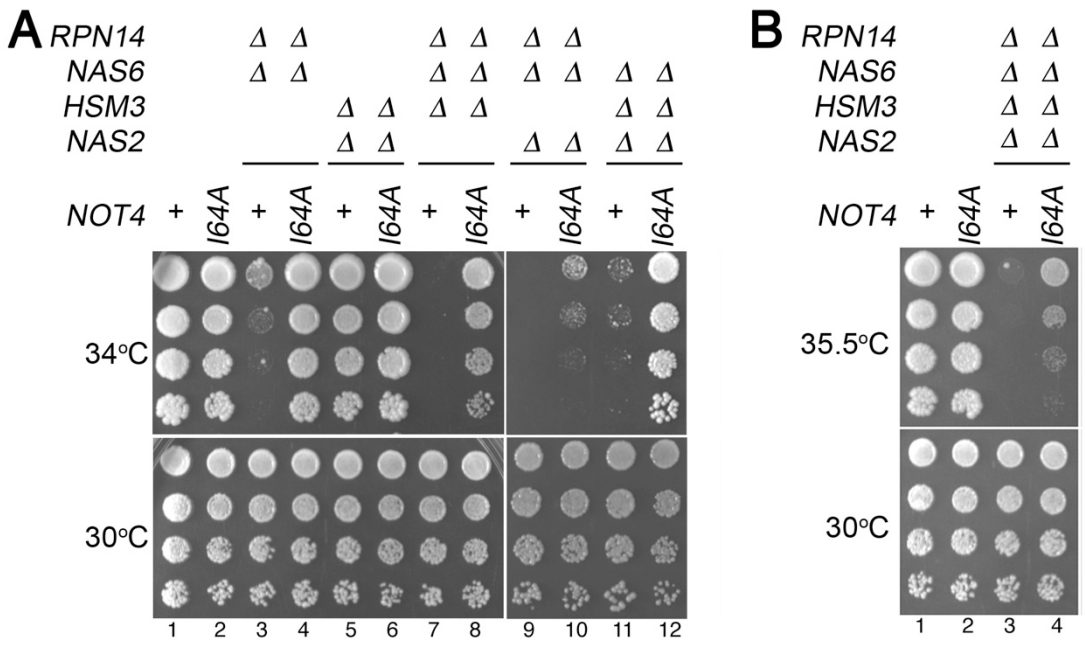

Fig. S2. The *not4-I64A* allele restores growth of the chaperone deletion mutants.

A, B, The *not4-I64A* allele, which specifically disables Not4 ubiquitin ligase activity like the *not4-L35A* allele, restores growth of the cells lacking multiple chaperones. Three-fold serial dilutions of the indicated yeast strains were spotted onto YPD plates and were grown at the indicated temperatures for 2-4 days. To assess growth phenotypes, we deleted multiple chaperones to eliminate functional redundancy among the chaperones; single chaperone deletion mutants do not exhibit noticeable growth phenotypes (1, 13, 14).

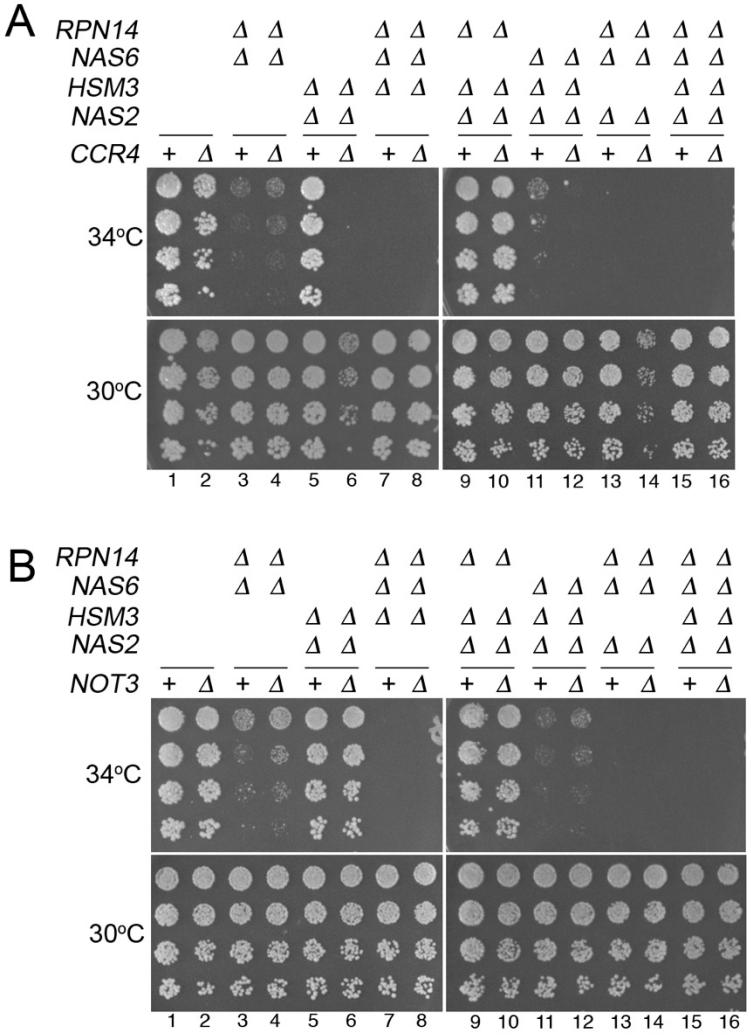

Fig. S3. Chaperone-mediated base assembly is regulated by Not4 ubiquitin ligase activity specifically, rather than by the general function of the Ccr4-Not complex.

A, Deletion of *CCR4*, a deadenylase subunit of the Ccr4-Not complex, does not suppress the phenotypes of the chaperone deletion mutants. Three-fold serial dilutions of the indicated yeast strains were spotted onto YPD plates and were grown at the indicated temperatures for 3 days. The *ccr4Δ* allele exacerbates the growth of *nas2Δhsm3Δ* (compare lane 5 to 6) and *rpn14Δnas6Δnas2Δ* (bottom, compare lane 13 to 14), reflecting additive defects from disrupting two distinct cellular processes: mRNA deadenylation and protein degradation, reflecting function of the Ccr4-Not complex and proteasome, respectively.

B, Deletion of *NOT3*, a subunit of the Ccr4-Not complex, does not suppress the phenotypes of chaperone deletion mutants. Experiments were conducted as described in (**A**). If Not4 functions as a part of the Ccr4-Not complex to regulate base assembly, deletion of other subunits of the Ccr4-Not complex should show a similar phenotype to the *not4-L35A* mutant—restoring growth of the chaperone mutants as shown in Fig 2. This is not the case, as shown by the results in (**A**) and (**B**). These data suggest that Not4-mediated regulation of proteasome assembly does not depend on the function of the Ccr4-Not complex, but on the ubiquitin ligase activity of Not4.

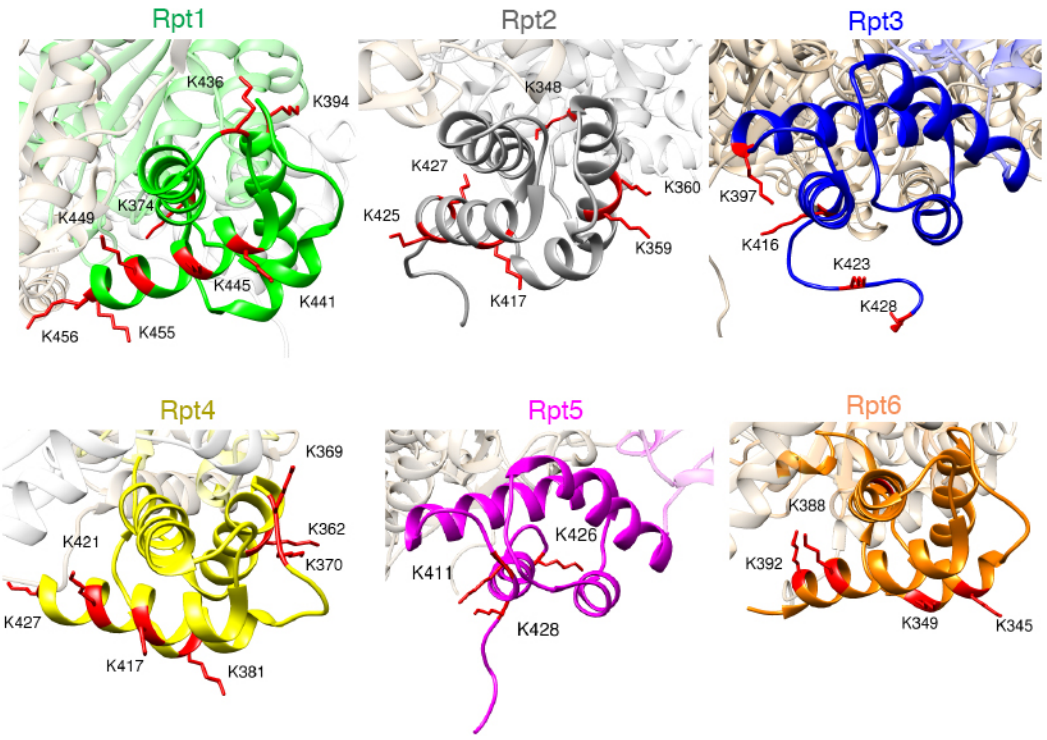

Fig. S4. Individual Rpt subunits exhibit similar numbers of surface lysines in the C-domain.

The C-domain of each Rpt subunit is shown in the known structure of the heterohexameric Rpt ring (PDB 4cr2) (15). Surface lysines are indicated and their side chains are shown in red. The images were generated using UCSF Chimera (16).

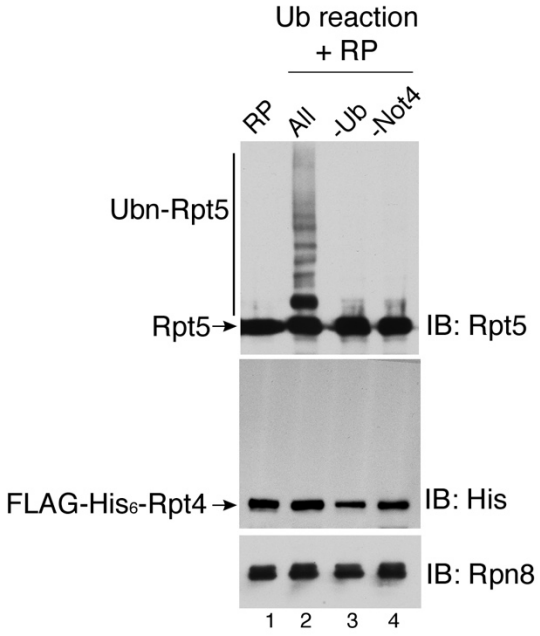

Fig. S5. In the RP, Rpt4 is not ubiquitinated by Not4, supporting that Rpt5 is the major ubiquitination target of Not4.

In vitro ubiquitination experiments confirming that Rpt4 is not a ubiquitination target of Not4 in the RP. Due to weak signal in our immunoblots for Rpt4 (Fig. 3B, lane 5-8) using an antibody against untagged Rpt4, we constructed N-terminally FLAG-His_6-tagged *RPT4* in its endogenous chromosomal locus. The RP was then purified, and *in vitro* ubiquitination was conducted as in Fig. 3B. Rpt4 detection through the His_6 tag generated a strong and specific signal, showing unmodified Rpt4 only (lane 2, middle panel). Polyubiquitinated Rpt5 is strongly detected, as shown in Fig. 3B (lane 2, top panel). Rpn8, a subunit of the RP, was used as a loading control.

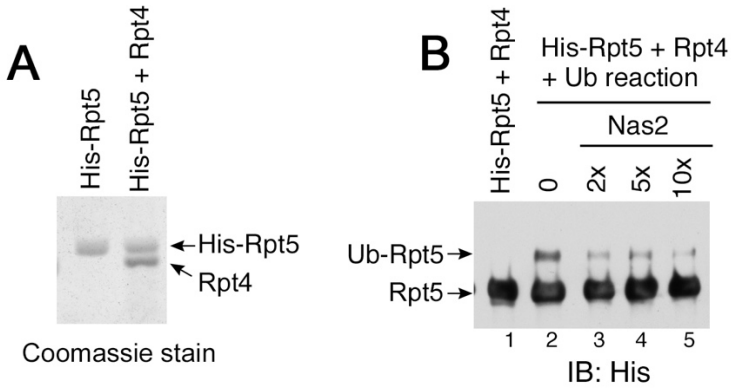

Fig. S6. Not4 ubiquitinates Rpt5 in the recombinant Rpt5-Rpt4 co-complex, and this ubiquitination is blocked by Nas2.

A, Affinity-purification of the recombinant Rpt5-Rpt4 co-complex. Full-length His_6-tagged Rpt5 was affinity-purified either alone (lane 1), or together with untagged full-length Rpt4 (lane 2) from *E. coli.* Purified proteins (2 μg) were resolved by 10% Bis-Tris SDS-PAGE and stained with Coomassie. In lane 2, Rpt5 and Rpt4 are detected at an approximate 1:1 stoichiometry, confirming the purification of Rpt5-Rpt4 co-complex.

B, Nas2 blocks Not4-mediated ubiquitination of Rpt5 in the Rpt5-Rpt4 co-complex. The Rpt5-Rpt4 co-complex (75 pmol) from ***A*** was subjected to *in vitro* ubiquitination as in Fig. 3A. Nas2 was added at the indicated molar excess to the Rpt5-Rpt4 co-complex for 10 min at room temperature first, prior to conducting the ubiquitination reaction for 30 min. The samples were then assessed by 10% Bis-Tris SDS-PAGE followed by immunoblotting for His-tagged Rpt5.

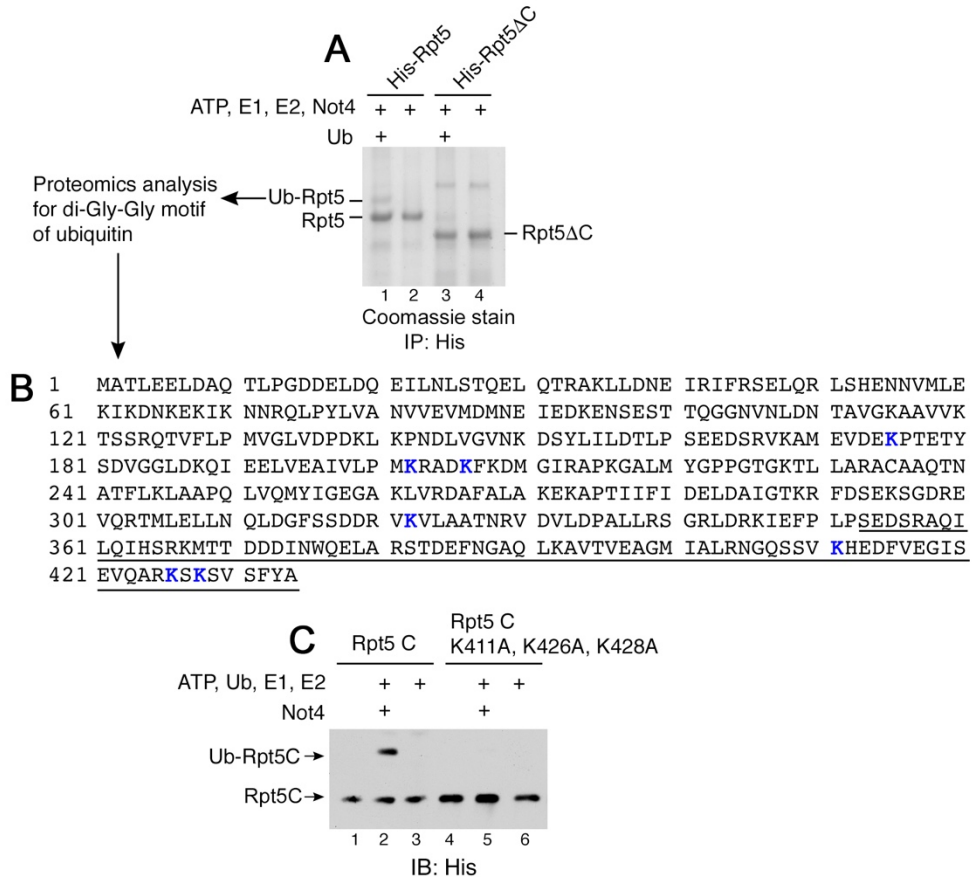

Fig. S7. Identification of Not4-mediated ubiquitination sites in the Rpt5 C-domain.

A, Recombinant His_6-Rpt5 or His_6-Rpt5ΔC was subjected to ubiquitination by Not4 *in vitro*, and was affinity-purified using metal affinity resin. Resin-bound materials were washed to eliminate all other ubiquitination reaction components, boiled, and analyzed by 10% Bis-Tris SDS-PAGE followed by Coomassie stain. Ubiquitinated Rpt5 band was then excised from the gel and subjected to mass spectrometry (see Supplementary Materials and Methods). Ubiquitin conjugation sites are known to harbor di-Gly-Gly signature, which derives from the C-terminus of ubiquitin (17).

B, Summary of the proteomics data for identification of ubiquitination sites in Rpt5. Amino acid sequence of Rpt5 is shown. Based on the proteomics data from ***A***, the Rpt5 C-domain (353-434, underlined) exhibited ubiquitination of three lysine residues (K411, K426, and K428; highlighted in blue) by Not4. Although several lysines in the AAA+ domain of Rpt5 (161-352) are also ubiquitinated (blue), they are unlikely to be major targets of Not4 since deletion of the C-domain alone substantially decreases Rpt5 ubiquitination by Not4 (see lane 3 in ***A***). Proteomics analysis was conducted twice using two independent samples.

C, Substitution of Not4 target lysines blocks ubiquitination of the Rpt5 C-domain. Ubiquitination was conducted using His_6-tagged Rpt5 C-domain vs. the mutant harboring indicated lysine-to-alanine substitutions for 1 hr at room temperature. To detect ubiquitinated species, samples were then analyzed by 10% Bis-Tris SDS-PAGE and immunoblotting with anti-His antibody.

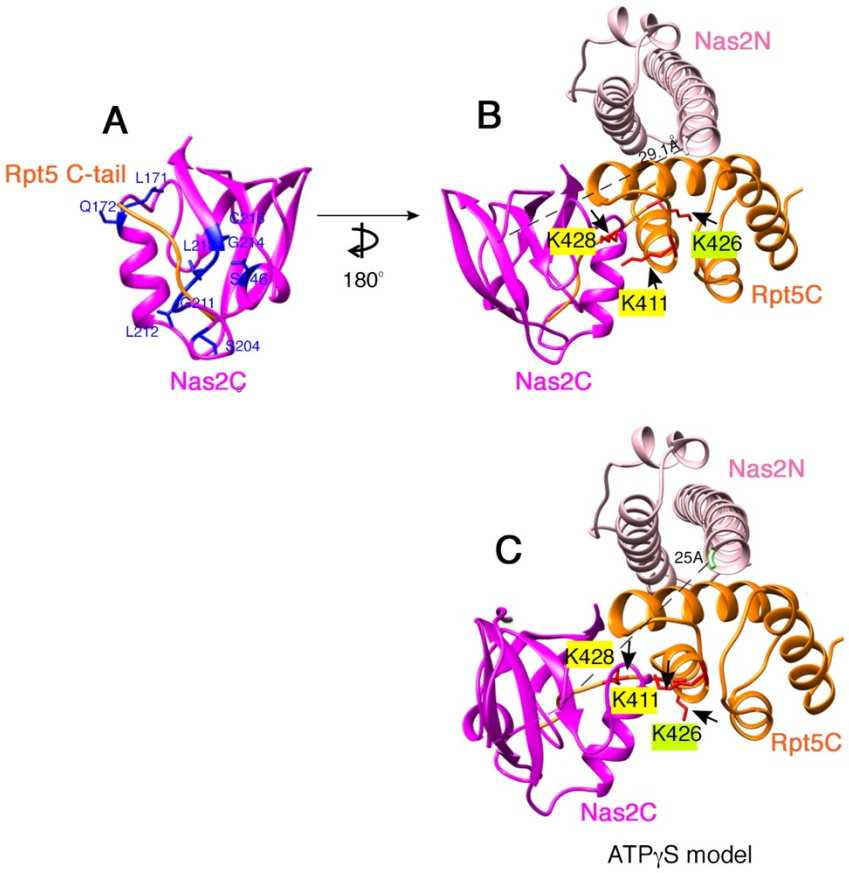

Fig. S8. Structural modeling of Nas2-Rpt5 co-complex.

A, B, Nas2 consists of N- and C-terminal domain, which are indicated as Nas2N (light pink, amino acids 1-120) (18) and Nas2C (magenta, amino acids 121-220) (19), respectively. As shown in the Nas2N-Rpt5C co-crystal structure (**B**, PDB 3WHL) (18), Nas2N does not obstruct Not4-targetted lysines in Rpt5. Instead, Nas2C obstructs K411 and K428 when modeled relative to Rpt5C as follows. We used the NMR chemical shift of Nas2C (blue highlighted amino acids) that is bound to the Rpt5 C-terminal heptapeptide (orange, ^{428}KSVSFYA^{434}) as shown in **A** from ref. (18, 19). The image in **A** was then positioned in the most likely orientation in **B**. Other orientations of Nas2C were eliminated because they are sterically incompatible with Nas2N or Rpt5C, conflicting with the experimental data that the extreme C-terminal end of the Rpt5 is required for Nas2 binding (20). Distance between M111 of Nas2N and Q129 of Nas2C (dotted line) is at 29.1Å (**B),** within the maximal distance (72Å) of the disordered linker (amino acids 112-128) between Nas2N and Nas2C. The images were generated using UCSF Chimera (16).

C, Structural modeling was done as described in **A** and **B**, except that the Rpt5C was modeled using the heterohexameric Rpt ring structure in the ATPγS-bound state (PDB 4CR4) (15). All three lysines (K411, K426, and K428) are occluded by Nas2C in this model. The ATPγS-bound state model mimics early stages of Rpt ring assembly, in which Rpt proteins bind ATP without hydrolysis (21, 22).

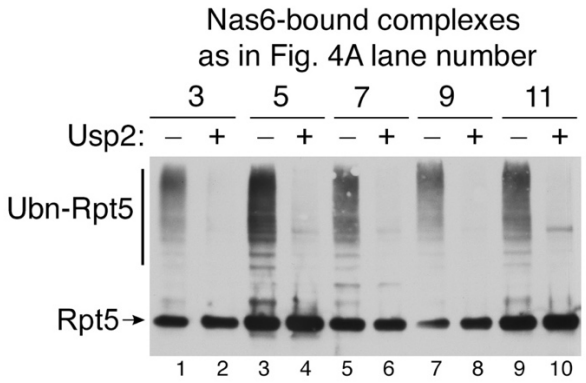

Fig. S9. Validation that high-molecular weight Rpt5 species are ubiquitinated Rpt5.

Nas6-bound assembly intermediates (1.5 μg), which correspond to the indicated lane in Fig. 4A, were incubated with a catalytic domain of Usp2, a deubiquitinase with broad specificity (23). The reactions were analyzed by 10% Bis-Tris SDS-PAGE and immunoblotting for Rpt5. Upon treatment with Usp2, all high-molecular Rpt5 species were no longer detected, indicating that they are indeed ubiquitinated Rpt5.

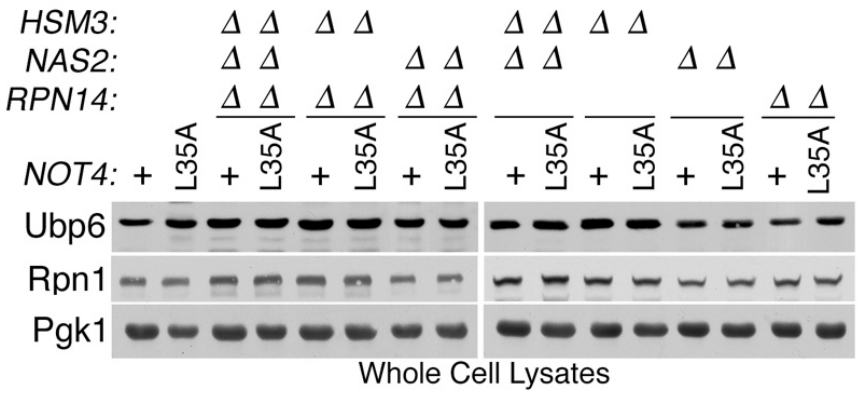

Fig. S10. Cellular abundance of Ubp6 and Rpn1 remains comparable in the chaperone mutants harboring Not4 vs. Not4-L35A catalytic mutant.

Whole cell lysates (20 μg) from the indicated strains were subjected to 10% Bis-Tris SDS-PAGE and immunoblotting for indicated proteins. These results confirm that changes in base-bound Ubp6 levels (Fig. 4A [iii]) do not reflect Ubp6 stability, but the extent of Ubp6 incorporation into the base via Not4-mediated control.

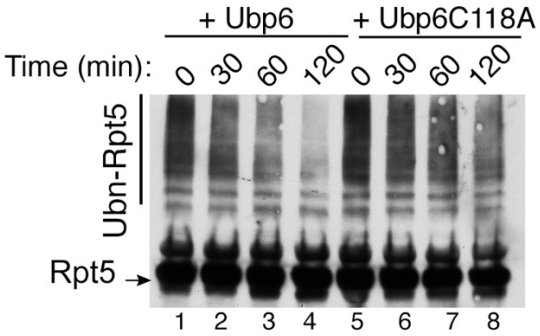

Fig. S11. *In vitro* deubiquitination assay suggesting that Ubp6 can deubiquitinate Rpt5 in the base assembly intermediates.

Since Ubp6 has been suggested to promote base assembly through its deubiquitinating activity (24), we tested whether Ubp6-base association can mediate Rpt5 deubiquitination. Nas6-bound assembly intermediates harboring ubiquitinated Rpt5 (Fig. 4A, lane 3) were mixed with either recombinant Ubp6 or its catalytic mutant, Ubp6-C118A, in excess to ensure their association with the base (See Supplementary Materials and Methods for detail). Samples were then subjected to 10% Bis-Tris SDS-PAGE and immunoblotting for Rpt5 to track ubiquitinated Rpt5. When Ubp6 was added, the polyubiquitin signal on Rpt5 was decreased in a time-dependent manner (lanes 1-4), but this signal remains largely unaffected when Ubp6-C118A is added (lanes 5-8). These results suggest that Ubp6 may deubiquitinate Rpt5 following its incorporation into the base, potentially providing a reversible mode of control on the progression of base assembly.

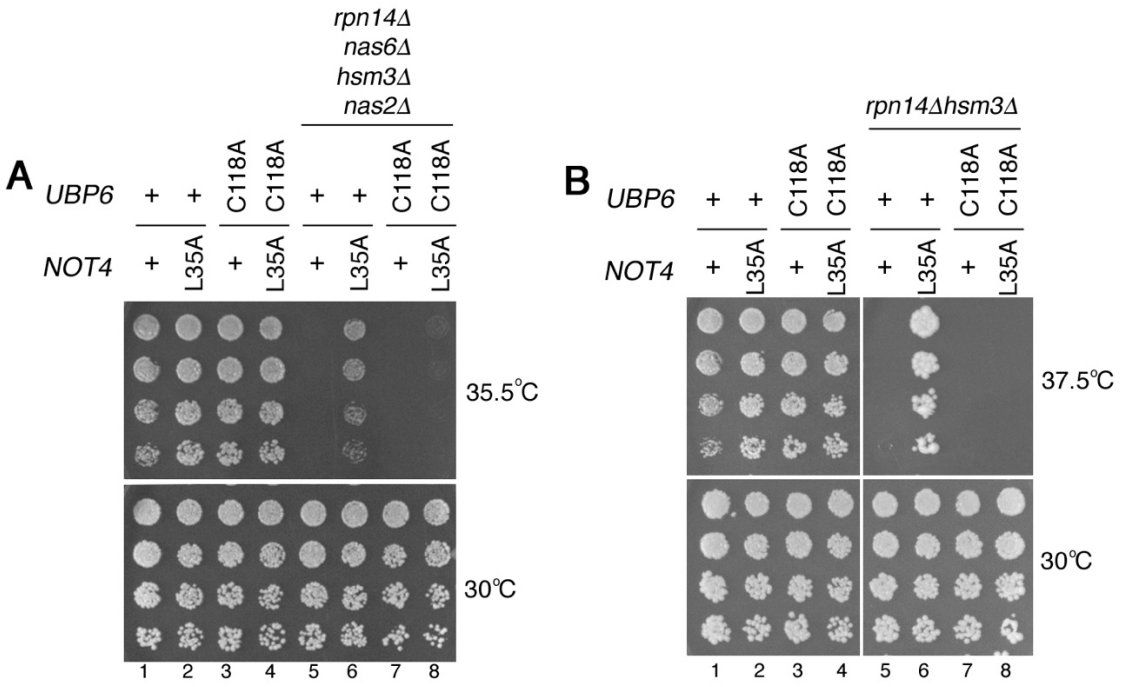

Fig. S12. Ubp6 activity is responsible for cell survival in the chaperone mutants expressing the *not4-L35A* allele.

A, B, Yeast growth assays showing that, upon expressing the *ubp6-C118A* mutant, the *not4-L35A* allele no longer restores growth of the chaperone mutants. Three-fold serial dilutions of indicated yeast cells were spotted onto YPD plates and were grown for 2-4 days at the indicated temperature. These results support our findings in Fig. 4C, that Ubp6's catalytic activity in restoring the free ubiquitin pool results in overall improvement of cell growth in the chaperone mutants expressing the *not4-L35A* allele (Fig. 2). These data support our model, in which Not4-mediated Rpt5 ubiquitination antagonizes Ubp6 activation when the heterohexameric Rpt ring assembly is defective, thereby blocking progression of base assembly.

Even when the level of base-bound Ubp6 seems to be similar between *rpn14Δhsm3Δ* and *rpn14Δhsm3Δnot4-L35A* (Fig. 4A, [iii], lanes 5, 6), Ubp6 activity is different between them. When Rpt5 is ubiquitinated (Fig. 4A [i], lane 5), Ubp6 remains inactive in the base since both Ubp6 and Ubp6-C118A exhibit the same phenotype in *rpn14Δhsm3Δ* cells (**B**, lanes 5, 7, top). When Rpt5 is not ubiquitinated (Fig. 4A [i], lane 6), Ubp6 is activated since the *ubp6-C118A* mutant abrogates cell growth of the *rpn14Δhsm3Δnot4-L35A* mutant (**B**, compare lane 6 to 8, top). Ubiquitinated Rpt5 might also disrupt the positioning of Ubp6 in the base, which is crucial for Ubp6 catalytic activity (25, 26).

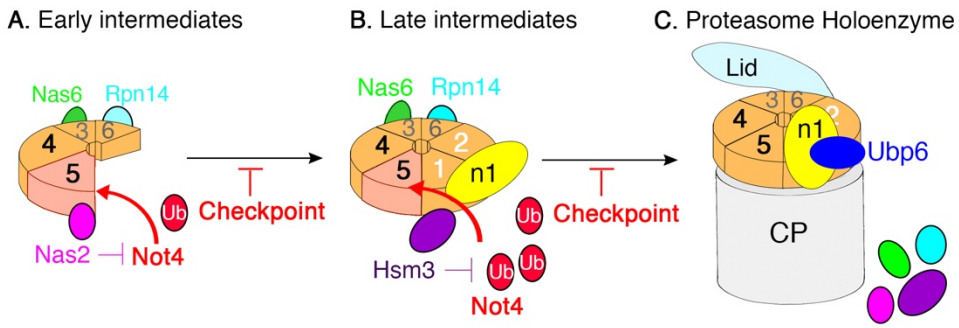

Fig. S13. A model for Not4-mediated checkpoint during chaperone-dependent proteasome assembly.

A, B, During proteasome assembly, hexameric Rpt ring (orange, numbers) assembles through step-wise addition of three Rpt-Rpt modules, as indicated in different font colors: grey, black, and white (14, 18, 27). In this process, Nas2 and Hsm3 sequentially obstruct Rpt5, restricting Not4's access to the ubiquitination sites in Rpt5. If assembly proceeds without these chaperones, due to chaperone deficiency or untimely assembly events, for example, Not4 can access Rpt5 and ubiquitinate it (red arrow). Ubiquitinated Rpt5 hinders subsequent incorporation of Rpn1 and Ubp6, thereby blocking progression of assembly process (checkpoint); see Discussion for details. When the chaperones can properly bind and act on these intermediates, assembly events proceed, permitting incorporation of Rpn1 and Ubp6 (**B, C**). Positioning of Rpn1 and Ubp6 in the base is further regulated during nucleotide-driven conformational changes as the heterohexameric Rpt ring matures into the proteasome holoenzyme (**B, C**) (22, 25, 26, 28).

C, Completion of the proteasome holoenzyme (lid-base-CP) leads to the eviction of the chaperones (1, 2, 22, 29). They can then be available for next round of proteasome assembly (**A, B**). For clarity, only representative assembly steps are shown, and other non-ATPase subunits (Rpn2 and Rpn13) are omitted.

Table S1. Identified peptides of the RP band as in Fig. 1B, lane 1.

	Gene name	No. peptides from RP
RP subunits	*RPN3*	10
	RPN5	10
	RPN6	8
	RPN7	10
	RPN8	7
	RPN9	8
	RPN11	10
	RPN12	4
	SEM1	1
	RPN10	1
	RPN1	14
	RPN2	28
	RPT1	14
	RPT2	10
	RPT3	3
	RPT4	7
	RPT5	6
	RPT6	13
	RPN13	3
	UBP6	3
Chaperones	*NAS6*	1
	NAS2	2

Table S2. Identified peptides of the base band as in Fig. 1B, lane 1.

	Gene name	No. of peptides from Base
Base subunits	*RPN1*	9
	RPN2	16
	RPT1	9
	RPT2	8
	RPT3	2
	RPT4	5
	RPT5	5
	RPT6	9
	RPN13	3
	UBP6	1
Chaperones	*NAS6*	1
	NAS2	2

Table S3. Yeast strains used in this study

Strain	Genotype	References
SUB62*	*MATa lys2-801 leu2-3, 2-112 ura3-52 his3-Δ200 trp1-1*	Ref.(30)
SP2406A	*MATa not4::NOT4-L35A (TRP1)*	This study
SP2345A	*MATa rpn14::hphMX nas6::HIS3*	This study
SP2434A	*MATa rpn14::hphMX nas6::HIS3 not4::NOT4-L35A (TRP1)*	This study
SP2497B	*MATa nas2::KAN hsm3::KAN*	Ref.(22)
SP2433A	*MATα nas2::KAN hsm3::KAN not4::NOT4-L35A (TRP1)*	This study
SP2377A	*MATα nas2::KAN hsm3::KAN rpn14::hphMX nas6::HIS3*	This study
SP2431A	*MATa nas2::KAN hsm3::KAN rpn14::hphMX nas6::HIS3 not4::NOT4-L35A (TRP1)*	This study
SP1655A	*MATa nas2::NAS2-6×Gly-3×FLAG (kanMX6)*	Ref.(22)
SP2664A	*MATa nas2::NAS2-6×Gly-3×FLAG (kanMX6) not4::NOT4-L35A (TRP1)*	This study
SP2665A	*MATα nas2::NAS2-6×Gly-3×FLAG (kanMX6) not4::NOT4-I64A (TRP1)*	This study
SP1687A	*MATα nas2::NAS2-6×Gly-3×FLAG (kanMX6) not4::KAN*	This study
sJR220A	*MATα rpn14::hphMX hsm3::KAN nas6::TRP1*	Ref.(1)
SP2432B	*MATa rpn14::hphMX hsm3::KAN nas6::TRP1 not4::NOT4-L35A (TRP1)*	This study
SP2501A	*MATa rpn14::hphMX hsm3::KAN nas2::KAN*	Ref.(22)
SP2448A	*MATa rpn14::hphMX hsm3::KAN nas2::KAN not4::NOT4-L35A (TRP1)*	This study
SP2500A	*MATa hsm3::KAN nas6::HIS3 nas2::KAN*	This study
SP2449A	*MATα hsm3::KAN nas6::HIS3 nas2::KAN not4::NOT4-L35A (TRP1)*	This study
SP2501A	*MATα rpn14::hphMX nas6::HIS3 nas2::KAN*	This study
SP2450A	*MATa rpn14::hphMX nas6::HIS3 nas2::KAN not4::NOT4-L35A (TRP1)*	This study
SP2407A	*MATα not4::NOT4-I64A(TRP1)*	This study
SP2427A	*MATa not4::NOT4-I64A(TRP1) nas2::KAN hsm3::KAN rpn14::hphMX nas6::HIS3*	This study
SP2428A	*MATα not4::NOT4-I64A(TRP1) hsm3::KAN rpn14::hphMX nas6::HIS3*	This study
SP2451A	*MATa not4::NOT4-I64A(TRP1) rpn14::hphMX nas6::HIS3 nas2::KAN*	This study
SP2440A	*MATa not4::NOT4-I64A(TRP1) hsm3::KAN nas6::HIS3 nas2::KAN*	This study
SP2438A	*MATα not4::NOT4-I64A(TRP1) hsm3::KAN rpn14::hphMX*	This study
SP2439A	*MATα not4::NOT4-I64A(TRP1) hsm3::KAN nas6::HIS3*	This study
SP2453A	*MATα not4::NOT4-I64A(TRP1) nas6::HIS3 nas2::KAN*	This study
SP2452A	*MATa not4::NOT4-I64A(TRP1) rpn14::hphMX nas2::KAN*	This study
YYS41	*MATa uba1::UBA1*^{3xFLAG} (W303-1A background)	Ref.(3)
TG931	*MATa rpt1::RPT1-TEV-ProA (HIS3)*	Ref.(29)
sDL133	*MATa rpn11::RPN11-TEV-ProA (HIS3)*	Ref.(31)
SP1677A	*MATa nas6::NAS6-6×Gly-*$^{3×FLAG}$*(hphMX)*	Ref.(22)
SP3128A	*MATα nas6::NAS6-6×Gly-3×FLAG(hphMX) rpn14::hphMX hsm3::KAN nas2::NAT*	This study
SP3126A	*MATa nas6::NAS6-6×Gly-3×FLAG(hphMX) rpn14::hphMX hsm3::KAN nas2::NAT NOT4-L35A(TRP1)*	This study
SP2692A	*MATa nas6::NAS6-6×Gly-3×FLAG(hphMX) rpn14::hphMX hsm3::KAN*	This study
SP2695A	*MATa nas6::NAS6-6×Gly-3×FLAG(hphMX) rpn14::hphMX hsm3::KAN not4::NOT4-L35A(TRP1)*	This study
SP3124A	*MATa nas6::NAS6-6×Gly-3×FLAG(hphMX) rpn14::hphMX nas2::NAT*	This study
SP3125A	*MATa nas6::NAS6-6×Gly-3×FLAG(hphMX) rpn14::hphMX nas2::NAT not4::NOT4-L35A(TRP1)*	This study

SP3127A	*MATa nas6::NAS6-6×Gly-3×FLAG(hphMX) hsm3::KAN nas2::NAT*	This study
SP3133A	*MATα nas6::NAS6-6×Gly-3×FLAG(hphMX) hsm3::KAN nas2::NAT not4::NOT4-L35A(TRP1)*	This study
SP3129A	*MATα nas6::NAS6-6×Gly-3×FLAG(hphMX) hsm3::KAN*	This study
SP3130A	*MATα nas6::NAS6-6×Gly-3×FLAG(hphMX) hsm3::KAN not4::NOT4-L35A(TRP1)*	This study
SP3132A	*MATα nas6::NAS6-6×Gly-3×FLAG(hphMX) nas2::NAT*	This study
SP3134A	*MATa nas6::NAS6-6×Gly-3×FLAG(hphMX) nas2::NAT not4::NOT4-L35A(TRP1)*	This study
SP1883A	*MATa nas6::NAS6-6×Gly-3×FLAG(hphMX) rpn14::hphMX*	This study
SP3131A	*MATa nas6::NAS6-6×Gly-3×FLAG(hphMX) rpn14::hphMX not4::NOT4-L35A(TRP1)*	This study
SP3305A	*MATa rpt5::rpt5-K411A, K426A, K428A (KanMX6) nas6::NAS6-6×Gly-3×FLAG(hphMX)*	This study
SP3306A	*MATa rpt5::rpt5-K411A, K426A, K428A (KanMX6) nas6::NAS6-6×Gly-3×FLAG(hphMX) not4::NOT4-L35A(TRP1)*	This study
SP3307A	*MATα rpt5::rpt5-K411A, K426A, K428A (KanMX6) nas6::NAS6-6×Gly-3×FLAG(hphMX) rpn14::hphMX nas2::NAT hsm3::KAN*	This study
SP3308A	*MATα rpt5::rpt5-K411A, K426A, K428A (KanMX6) nas6::NAS6-6×Gly-3×FLAG(hphMX) rpn14::hphMX nas2::NAT hsm3::KAN not4::NOT4-L35A(TRP1)*	This study
SP3372A	*MATa rpt5::rpt5-K411A, K426A, K428A (KanMX6) nas2::NAT nas6::NAS6-6×Gly-3×FLAG(hphMX)*	This study
SP3373B	*MATa rpt5::rpt5-K411A, K426A, K428A (KanMX6) nas2::NAT nas6::NAS6-6×Gly-3×FLAG(hphMX) not4::NOT4-L35A(TRP1)*	This study
sJR287	*MATα rpn4::KanMX6*	This study
SP1658C	*MATa not4:: KanMX6*	This study
SP2186A	*MATa not4:: KanMX6 rpn4::KanMX6*	This study
SP2246A	*MATa ccr4::KanMX6*	This study
SP3430A	*MATα ccr4::KanMX6 rpn14::hphMX nas6::HIS3*	This study
SP3422	*MATa ccr4::KanMX6 hsm3::KAN nas2::NAT*	This study
SP3419A	*MATα ccr4::KanMX6 rpn14::hphMX nas6::HIS3 hsm3::KAN*	This study
SP3420A	*MATa ccr4::KanMX6 rpn14::hphMX hsm3::KAN nas2::NAT*	This study
SP3421A	*MATa ccr4::KanMX6 nas6::HIS3 hsm3::KAN nas2::NAT*	This study
SP3428	*MATα ccr4::KanMX6 rpn14::hphMX nas6::HIS3 nas2::NAT*	This study
SP3418	*MATa ccr4::KanMX6 rpn14::hphMX nas6::HIS3 hsm3::KAN nas2::NAT*	This study
SP2248A	*MATa not3::KanMX6*	This study
SP3426	*MATa not3::KanMX6 rpn14::hphMX nas6::HIS3*	This study
SP3427	*MATa not3::KanMX6 hsm3::KAN nas2::NAT*	This study
SP3423A	*MATa not3::KanMX6 rpn14::hphMX nas6::HIS3 hsm3::KAN*	This study
SP3424	*MATa not3::KanMX6 rpn14::hphMX hsm3::KAN nas2::NAT*	This study
SP3425	*MATa not3::KanMX6 nas6::HIS3 hsm3::KAN nas2::NAT*	This study
SP3429	*MATa not3::KanMX6 rpn14::hphMX nas6::HIS3 nas2::NAT*	This study
SP3492A	*MATa not3::TRP1 rpn14::hphMX nas6::HIS3 hsm3::KAN nas2::NAT*	This study
SP3299B	*MATα rpt4::FLAG-HIS$_6$-RPT4 (KanMX6) rpn11::RPN11-TEV-ProA (HIS3)*	This study

*All strains are congenic to SUB62 background unless indicated otherwise.

Table S4. *E. coli* plasmids used in this study

Name	Plasmid description	Reference
pJR56	GST-Rpn14 in pGEX-6P-1	Ref.(1)
pJR40	GST-Nas6 in pGEX-6P-1	Ref.(1)
pJR89	GST-Hsm3 in pGEX-6P-1	Ref.(1)
pSP128	GST-Nas2 in pGEX-6P-1	This study
pSP157	GST-Ubc4 in pGEX-6P-1	Ref.(3)
pSP58	GST-Not4 in pGEX-6P-1	This study
pJR168	His_6-Rpt5 C-domain (353-434 amino acids) in pRSF-Duet-1	Ref.(20)
pSP151	His_6-Rpt5 full-length in pRSF-Duet-1	This study
pSP152	His_6-Rpt5ΔC (1-352 amino acids) in pRSF-Duet-1	This study
pSP158	Untagged Rpt4 in pRSF-Duet-1	This study
pSP153	His_6-Rpt5 C-domain (K411A, K426A, K428A) in pRSF-Duet-1	This study
pJR165	His_6-Rpt1 C-domain (381-467 amino acids) in pRSF-Duet-1	Ref.(1)

REFERENCES

1. Roelofs J*, et al.* (2009) Chaperone-mediated pathway of proteasome regulatory particle assembly. *Nature* 459(7248):861-865.
2. Park S*, et al.* (2009) Hexameric assembly of the proteasomal ATPases is templated through their C termini. *Nature* 459(7248):866-870.
3. Saeki Y, Tayama Y, Toh-e A, & Yokosawa H (2004) Definitive evidence for Ufd2-catalyzed elongation of the ubiquitin chain through Lys48 linkage. *Biochem Biophys Res Commun* 320(3):840-845.
4. Hanzawa H*, et al.* (2001) The structure of the C4C4 ring finger of human NOT4 reveals features distinct from those of C3HC4 RING fingers. *J Biol Chem* 276(13):10185-10190.
5. Hanssum A*, et al.* (2014) An inducible chaperone adapts proteasome assembly to stress. *Mol Cell* 55(4):566-577.
6. Suraweera A, Munch C, Hanssum A, & Bertolotti A (2012) Failure of amino acid homeostasis causes cell death following proteasome inhibition. *Mol Cell* 48(2):242-253.
7. Shevchenko A, Tomas H, Havlis J, Olsen JV, & Mann M (2006) In-gel digestion for mass spectrometric characterization of proteins and proteomes. *Nat Protoc* 1(6):2856-2860.
8. Cox J & Mann M (2008) MaxQuant enables high peptide identification rates, individualized p.p.b.-range mass accuracies and proteome-wide protein quantification. *Nat Biotechnol* 26(12):1367-1372.
9. Hanna J*, et al.* (2006) Deubiquitinating enzyme Ubp6 functions noncatalytically to delay proteasomal degradation. *Cell* 127(1):99-111.
10. Preissler S*, et al.* (2015) Not4-dependent translational repression is important for cellular protein homeostasis in yeast. *EMBO J*.
11. Mannhaupt G, Schnall R, Karpov V, Vetter I, & Feldmann H (1999) Rpn4p acts as a transcription factor by binding to PACE, a nonamer box found upstream of 26S proteasomal and other genes in yeast. *FEBS Lett* 450(1-2):27-34.
12. Xie Y & Varshavsky A (2001) RPN4 is a ligand, substrate, and transcriptional regulator of the 26S proteasome: a negative feedback circuit. *Proc Natl Acad Sci U S A* 98(6):3056-3061.
13. Funakoshi M, Tomko RJ, Jr., Kobayashi H, & Hochstrasser M (2009) Multiple assembly chaperones govern biogenesis of the proteasome regulatory particle base. *Cell* 137(5):887-899.
14. Saeki Y, Toh EA, Kudo T, Kawamura H, & Tanaka K (2009) Multiple proteasome-interacting proteins assist the assembly of the yeast 19S regulatory particle. *Cell* 137(5):900-913.
15. Unverdorben P*, et al.* (2014) Deep classification of a large cryo-EM dataset defines the conformational landscape of the 26S proteasome. *Proc Natl Acad Sci U S A* 111(15):5544-5549.
16. Pettersen EF*, et al.* (2004) UCSF Chimera--a visualization system for exploratory research and analysis. *J Comput Chem* 25(13):1605-1612.
17. Peng J*, et al.* (2003) A proteomics approach to understanding protein ubiquitination. *Nat Biotechnol* 21(8):921-926.

18. Satoh T*, et al.* (2014) Structural basis for proteasome formation controlled by an assembly chaperone nas2. *Structure* 22(5):731-743.
19. Singh CR*, et al.* (2014) 1.15 A resolution structure of the proteasome-assembly chaperone Nas2 PDZ domain. *Acta Crystallogr F Struct Biol Commun* 70(Pt 4):418-423.
20. Lee SY, De la Mota-Peynado A, & Roelofs J (2011) Loss of Rpt5 protein interactions with the core particle and Nas2 protein causes the formation of faulty proteasomes that are inhibited by Ecm29 protein. *J Biol Chem* 286(42):36641-36651.
21. Thompson D, Hakala K, & DeMartino GN (2009) Subcomplexes of PA700, the 19 S regulator of the 26 S proteasome, reveal relative roles of AAA subunits in 26 S proteasome assembly and activation and ATPase activity. *J Biol Chem* 284(37):24891-24903.
22. Li F*, et al.* (2017) Nucleotide-dependent switch in proteasome assembly mediated by the Nas6 chaperone. *Proc Natl Acad Sci U S A* 114(7):1548-1553.
23. Besche HC*, et al.* (2014) Autoubiquitination of the 26S proteasome on Rpn13 regulates breakdown of ubiquitin conjugates. *EMBO J* 33(10):1159-1176.
24. Sakata E*, et al.* (2011) The catalytic activity of Ubp6 enhances maturation of the proteasomal regulatory particle. *Mol Cell* 42(5):637-649.
25. Aufderheide A*, et al.* (2015) Structural characterization of the interaction of Ubp6 with the 26S proteasome. *Proc Natl Acad Sci U S A* 112(28):8626-8631.
26. Bashore C*, et al.* (2015) Ubp6 deubiquitinase controls conformational dynamics and substrate degradation of the 26S proteasome. *Nat Struct Mol Biol* 22(9):712-719.
27. Tomko RJ, Jr., Funakoshi M, Schneider K, Wang J, & Hochstrasser M (2010) Heterohexameric ring arrangement of the eukaryotic proteasomal ATPases: implications for proteasome structure and assembly. *Mol Cell* 38(3):393-403.
28. Lu Y*, et al.* (2017) Conformational Landscape of the p28-Bound Human Proteasome Regulatory Particle. *Mol Cell* 67(2):322-333 e326.
29. Park S*, et al.* (2013) Reconfiguration of the proteasome during chaperone-mediated assembly. *Nature* 497(7450):512-516.
30. Finley D, Ozkaynak E, & Varshavsky A (1987) The yeast polyubiquitin gene is essential for resistance to high temperatures, starvation, and other stresses. *Cell* 48(6):1035-1046.
31. Leggett DS*, et al.* (2002) Multiple associated proteins regulate proteasome structure and function. *Mol Cell* 10(3):495-507.